U.F.S. EDITION

SEXA CORPUS

U.F.S. Publishing (Unified Field Systems LLC)

A U.F.S. EDITION · ONE PAPER, ONE BOOK

SEXA CORPUS · W004

HEXAD Intercept Symmetry–Telemetry under RICOLMC-DDF Γ-Gated Resource Completeness

Upgrading the Last Constant's Quaternionic Expansion Equation to Six-Planet Tracking — A U.F.S Pre-Registration Locked Before the Data Arrive

Jered McClain · Erydir Ceisiwr · Jonathan McDaniel

2026

OSF preprint; not peer reviewed; pre-registration locked

DOI 10.17605/OSF.IO/C32NZ

U.F.S.
UNIFIED FIELD SYSTEMS

"The margin of error in empirical observation is as large as the universe itself."

U.F.S. PUBLISHING · EDITION COPY · UNIFIED FIELD SYSTEMS LLC
OSF preprint · DOI 10.17605/OSF.IO/C32NZ

DOI 10.17605/OSF.IO/C32NZ
https://doi.org/10.17605/OSF.IO/C32NZ

U.F.S. EDITION
U.F.S. PUBLISHING · EDITION COPY · UNIFIED FIELD SYSTEMS LLC
OSF preprint · DOI 10.17605/OSF.IO/C32NZ
DOI SEAL
DOI 10.17605/OSF.IO/C32NZ
https://doi.org/10.17605/OSF.IO/C32NZ

HEXAD Intercept Symmetry–Telemetry under RICOLMC-DDF Γ-Gated Resource Completeness: Upgrading the Last Constant's Quaternionic Expansion Equation to Six-Planet Tracking

A U.F.S Pre-Registration Locked Before the Data Arrive

Jered McClain* Erydir Ceisiwr†

Jonathan McDaniel‡

Unified Field Systems LLC, https://www.unifiedfieldsystems.com/

11 November 2026

Version 5 (9D SREF (SREF-EX9D) root equation and 5D YYQPA-SEXA seed reproduced; U.F.S. CAT and human-in-the-loop definitions added; pre-registration unchanged from v3/v4; primary $k = 3$ gates).

Preprint; not peer reviewed

Abstract

The Trump Constant expansion equation, now called the Last Constant equation, was written for a single observer seated on a "quaternionic park bench" with four perspectives: the universe as manifold, its light, the Empire Wave, and the background radiation [9]. We upgrade the observer from that single quaternion frame to the six-gate HEXAD tracking system (Mercury, Earth, Jupiter, Saturn, Uranus, Neptune) [14]. The upgrade multiplies the 2880-D expansion speed by a tracking factor $\mathcal{H}_6(t)$, the geometric mean of the six gate-quaternion norms. We prove that after admissibility enforcement $\mathcal{H}_6 \equiv 1$, so the new equation reduces exactly to the quaternion form. We call this condition, in which the six gate intercepts agree and $\mathcal{H}_6 \equiv 1$, *HEXAD Intercept Symmetry*. Before enforcement $\log \mathcal{H}_6$ is a measurable observer-drift statistic, which gives concrete form to the original paper's "real-time observer error correction". We lock a complete pre-registration before BepiColombo science-phase data exist. The primary scored test uses the $k = 3$ gates with public daily observational data in 2027–28 (Mercury: BepiColombo magnetometers; Earth: Arase radiation-belt fluxes; Jupiter: Nançay decametric radio), with locked observables, a circular-shift surrogate null, a solar-rotation robustness check, $\alpha = 0.01$ and a three-way decision rule. The full six-gate test is a secondary analysis that activates only if Saturn, Uranus and Neptune data exist. Items that would require new physics are declared OPEN and are not scored. A new section maps the six gates and the enforcement step onto the RICOLMC-DDF six-glyph Γ gate, its completeness clauses (C1)–(C4) and the 9D SREF (SREF-EX9D) root equation, frozen at v1.4, preceded by the 5D YYQPA-SEXA seed, as a structural correspondence only, reading $\mathcal{H}_6 \equiv 1$ as the gate passing on all six gates [15, 11]. The same section records two U.F.S. definitions used here and not drawn from RICOLMC-DDF, CAT and human-in-the-loop, which add no scored test. A synthetic dry run returns CONFIRM, REFUTE and NO DECISION in the intended cases. Nothing here solves gravity: the internal scoreboard remains 6.75/19.

*Bronx, NY, USA; ORCID 0009-0005-6185-3749; jered@unifiedfieldsystems.com

†Gower, South Wales, UK; ORCID 0009-0004-4577-5253; erydir@unifiedfieldsystems.com

‡Carthage, TX, USA; ORCID 0009-0004-1239-6855; jonathan@unifiedfieldsystems.com

U.F.S. EDITION
DOI SEAL
U.F.S. PUBLISHING · EDITION COPY · UNIFIED FIELD SYSTEMS LLC
OSF preprint · DOI 10.17605/OSF.IO/C32NZ
DOI 10.17605/OSF.IO/C32NZ
https://doi.org/10.17605/OSF.IO/C32NZ

1 Motivation

From one bench to six gates. The original paper [9] argued that "the margin of error of empirical observation is as large as the universe itself," and that embedding four quaternionic observer perspectives in SEXA mathematics stabilises the observer logic matrix. That observer is one point: every reading of the expansion is taken from a single frame, and nothing inside the equation checks that frame against another. The HEXAD layer [14] already assigns a quaternionic check-in gate to each of six bodies. Using those six gates as the observer gives the equation an internal cross-check: if the six frames agree, the observer is consistent; if they drift apart, the drift is visible and correctable.

Origin of the Empire Wave speed question. The question this equation answers, namely how fast the universe's outward expansion runs compared with light, was crystallised for the lead author by an unresolved exchange in a 2017 Quantum Gravity Research talk [19]. At about 1:11:14, Klee Irwin asks whether expansion is currently outpacing light ("is there expansion faster now or no?"). Jack Sarfatti answers that there is no limitation on the speed of the expansion of space, only on particles moving within space, and sets the point aside. The two never reach agreement. That open question is what led to the Empire Wave speed and the Trump Constant, now the Last Constant. We thank Klee Irwin for creating, conceptualising and guiding the Empire Wave, as the original paper does.

Status vocabulary. We follow [14]: DEFINED (locked in the corpus), PROVED (follows from definitions here), ASSUMED, PROPOSED, OPEN, LOCKED (fixed by this pre-registration), and SYNTHETIC (simulated, not data).

2 The equation

The original 2880-D form [9, 14] is

$$V_{\text{univ}}^{(2880)}(t,\phi) = C_T\Big(\prod_{\ell=5}^{2880}\frac{\Psi_\ell}{\phi_\ell^2}\Big)^{\frac{1}{2880-4}}\cdot 60^{\bar{n}}, \qquad \bar{n} = \frac{1}{2880-4}\sum_{\ell=5}^{2880} n_\ell. \tag{1}$$

The HEXAD form, with C_T renamed C_L, is

$$\boxed{V_{\text{univ},\mathcal{H}}^{(2880)}(t,\phi) = C_L\Big(\prod_{\ell=5}^{2880}\frac{\Psi_\ell}{\phi_\ell^2}\Big)^{\frac{1}{2880-4}}\cdot 60^{\bar{n}}\cdot \mathcal{H}_6(t)} \tag{2}$$

$$\mathcal{H}_6(t) = \Big(\prod_{p=1}^{6}\|q_p(t)\|\Big)^{1/6}, \qquad q_p(t) = q_{p,0} + q_{p,1}\,i + q_{p,2}\,j + q_{p,3}\,k. \tag{3}$$

What the four original perspectives become. The four perspectives of [9] were properties of one observer. In the HEXAD form each gate carries its own four-slot quaternion, so the single four-perspective observer becomes six four-slot observers whose agreement is summarised by one number, $\mathcal{H}_6$. Whether the four Earth windows can be identified one-to-one with the original four perspectives (manifold, light, Empire Wave, background radiation) is OPEN; we do not assume it.

Symbol	Meaning and status
$V^{(2880)}_{\text{univ},\mathcal{H}}$	Outward expansion speed in the 2880-D SEXA stack, tracked from six gates.
C_L	Last Constant (formerly Trump Constant C_T). Bridge $V_{\text{Last}}/c = (C_{EW}/c)\,60^{\bar{n}}$ with target 10^{19} [14, 23]; target, not measurement.
$\Psi_\ell,\ \phi_\ell$	Payload (energy density) and coordinate scaling of dimension ℓ; per-dimension values for $\ell = 5, \ldots, 2880$ OPEN.
$1/(2880-4)$	Geometric average over the 2876 higher fields.
$60^{\bar{n}}$	Sexagesimal harmonic scaling; $\bar{n} = 10$ is fit-adopted, not derived [14].
$\mathcal{H}_6(t)$	HEXAD tracking factor, geometric mean of six gate-quaternion norms (this paper).
$q_p(t)$	Gate state at body p. Earth: PRE/OUTER/INNER/POST $\to (q_0,q_1,q_2,q_3)$; other bodies: in/out $\to (q_0,q_1)$, $q_2 = q_3 = 0$ [14, 22].
q_{Moon}	Null control: $\|q_{\text{Moon}}\| = 1$ identically; not a factor in $\mathcal{H}_6$.

Table 1: Legend for Eqs. (2)–(3). Gate list and window mapping are ASSUMED as in [14].

p	Body	Windows $\to$ components	Lane
1	Mercury	in/out $\to (q_0,q_1)$ (weak field)	UFS
2	Earth	PRE/OUTER/INNER/POST $\to (q_0,q_1,q_2,q_3)$	Vespar
3–6	Jupiter, Saturn, Uranus, Neptune	in/out $\to (q_0,q_1)$	UFS
–	Moon	none (no global belt): null control	–

Table 2: The six HEXAD tracking points.

3 Reduction and invariance

Definition 1 (Enforcement)**.** *Following the AMN Authority Tensor [13], admissibility enforcement maps a nonzero gate state to the unit sphere, $\mathcal{E}(q) = q/\|q\|$, and admissible updates act by unit-quaternion rotation.*

Theorem 1 (Exact reduction; PROVED)**.** *If every gate is enforced, $\|q_p\| = 1$ for $p = 1, \ldots, 6$, then $\mathcal{H}_6(t) = 1$ and Eq. (2) equals Eq. (1) with $C_L = C_T$.*

Proof. $\mathcal{H}_6 = (\prod_p 1)^{1/6} = 1$, and the remaining factors of (2) are identical to those of (1). Partially populated gates ($q_2 = q_3 = 0$) have $\|q\| = \sqrt{q_0^2 + q_1^2}$, which enforcement also sets to 1. □

Proposition 1 (Rotation invariance; PROVED)**.** *For unit quaternions u_p, w_p, replacing $q_p \mapsto u_p\, q_p\, w_p$ leaves $\mathcal{H}_6$ unchanged.*

Proof. The quaternion norm is multiplicative, $\|uqw\| = \|u\|\|q\|\|w\| = \|q\|$. □

Proposition 1 means admissible AMN rotations never move $\mathcal{H}_6$; only norm-changing residuals, which enforcement would remove, register as drift.

Proposition 2 (Drift statistic; PROVED)**.** *Write $\|q_p\| = 1 + \delta_p$. Then*

$$D(t) \equiv \log \mathcal{H}_6(t) = \frac{1}{6}\sum_{p=1}^{6} \log(1+\delta_p) = \bar{\delta} - \tfrac{1}{2}\overline{\delta^2} + O(\delta^3), \tag{4}$$

and $V_{\mathcal{H}} = V_{\text{quat}}\, e^{D}$, so the fractional correction to the expansion speed is D to first order.

Proof. Take logarithms of (3) and Taylor-expand $\log(1+x)$. □

U.F.S. PUBLISHING · EDITION COPY · UNIFIED FIELD SYSTEMS LLC
OSF preprint · DOI 10.17605/OSF.IO/C32NZ
DOI 10.17605/OSF.IO/C32NZ
https://doi.org/10.17605/OSF.IO/C32NZ

Moon check. Because the Moon has no global belt, its gate has no windows to populate and is defined with $\|q_{\text{Moon}}\| = 1$. Any computed $\|q_{\text{Moon}}\| \neq 1$ therefore indicates a pipeline error, not physics. It verifies the tracker; it carries no information about expansion.

4 RICOLMC-DDF Γ-gated resource completeness of the HEXAD frame

This section places the HEXAD frame inside the RICOLMC-DDF completeness program [15]. It uses only definitions that appear in that deposit (page numbers are PDF pages of the 99-page OSF file) and follows the mapping already given in the U.F.S addendum [11]. Every correspondence here is *structural (definitional)*. It adds no new scored test, no new parameter, and changes no locked observable, window, null, threshold or decision rule of Section 5.

Locked name, gate and clauses. The locked program name of RICOLMC-DDF is "Recursive Interdomain Computational Omni-Logic embedding Monster–Moonshine Constrained Admissibility Manifold Completeness across Density, Dimension, Field, Liquidity, and Recursive Resource Completeness for Γ-Gated Resource Flows" [15, p. 15]. Its gate is the ordered six-glyph composition "$\Gamma := \bigcirc \circ \nabla \circ \mathrm{K} \circ \sigma \circ \mu \circ \mathbb{W} = \mathrm{Orr} \circ \mathrm{Na} \circ \mathrm{Ka} \circ \mathrm{Sa} \circ \mathrm{Mu} \circ \mathrm{Wa}$, acting right to left ($\mathbb{W} = \mathrm{Wa}$ first) … A configuration Ξ is Γ-admissible if $\Gamma(\Xi) = \Xi$" (Def. 11.3, p. 35), run as "an ordered fail-any procedure" (p. 18). Completeness is Def. 6.1 (p. 15): for every admissible encoded input, (C1) (executable) "$\mathcal{E}$ halts on $e_k(x)$ and returns a value of E_{SREF}"; (C2) (admissible under reduction) "$R(e_k(x)) \in \mathrm{Fix}(\Gamma_5)$"; (C3) (reconstructable) "there is a map e_k^{-1} on the image with $e_k^{-1}(e_k(x)) = x$"; (C4) (DDF-resolved) "the value returned in (C1) decomposes into sector terms, each with a density, a dimension index and a field label". Resources "are admissible only when Γ passes" (p. 15), and "Completeness in the title is definitional and locked. Instantiation for each domain is a separate theorem obligation" (p. 15).

HEXAD Intercept Symmetry as the Γ gate passing. We read enforcement $\mathcal{E}(q_p) = q_p/\|q_p\|$ on each gate as the admission step, and $\mathcal{H}_6 \equiv 1$ (HEXAD Intercept Symmetry, Theorem 1) as the Γ gate passing on all six gates at once. Fail-any semantics corresponds to the existing void-day rule: one Moon-check failure voids the day. This is a reading of the gate's *admission semantics*, not an identification of the six glyphs with the six planets. RICOLMC-DDF itself leaves the map from individual glyphs onto parts of its energy body open (O12, p. 54), so we supply none. Two source flags carry over [11]. The Critical-Line Theorem III.14 product $M_k = T_{\mathbb{W}} T_\mu(k) T_\sigma T_\kappa T_\nabla T_\bigcirc$ [12] applies Orr first, while RICOLMC Γ applies Wa first. The orders are reversed, and "order matters" (p. 36), so we note the difference and do not resolve it. Also, RICOLMC writes the Empire Wave Constant as $C_\Omega = \sqrt{720} \approx 26.833$, "a pure number" (p. 10).

U.F.S. PUBLISHING · EDITION COPY · UNIFIED FIELD SYSTEMS LLC
OSF preprint · DOI 10.17605/OSF.IO/C32NZ
DOI 10.17605/OSF.IO/C32NZ
https://doi.org/10.17605/OSF.IO/C32NZ

Clause	RICOLMC-DDF meaning	HEXAD counterpart (already in this paper)	Status
$\Gamma(\Xi) = \Xi$	ordered fail-any gate	enforcement on all gates, $\mathcal{H}_6 \equiv 1$; void day on any Moon-check failure	PROVED, LOCKED
(C1)	evaluation halts with a value	locked analysis runs once, by 31 Dec 2029, or returns NO DECISION	LOCKED
(C2)	reduction commutes with admission	enforcement then reduction gives the quaternion form (Theorem 1); in RICOLMC-DDF, $R \circ \Gamma_{2880} = \Gamma_5 \circ R$ is OPEN (O21, p. 15)	proved here / open there
(C3)	reconstructable encoding	seeded surrogates (20261111), SHA-256 hashes, public data DOIs	LOCKED
(C4)	sector-resolved value	$D = \frac{1}{k}\sum_p a_p$ resolves by gate (a gate label, not a density/field decomposition)	PROPOSED
resource flow	admitted only if Γ passes	telemetry enters ρ only on valid, non-void days	PROPOSED

Table 3: RICOLMC-DDF Γ gate and completeness clauses read onto the HEXAD frame (structural correspondence, following [11]).

4.1 The 9D SREF root equation (SREF-EX9D, frozen v1.4)

The 5D YYQPA-SEXA seed. RICOLMC-DDF takes SREF-EX9D as the energy body that extends a five-dimensional sketch: "The published JAM 9887 used a five-dimensional sketch, (2), as its energy body. The energy body the authors have since established is SREF-EX9D, frozen at version v1.4" (Section 13, printed p. 49, PDF p. 52) [15]. That published sketch (2) is not identical to the corpus 5D operating display line. The 5D YYQPA-SEXA seed, reproduced exactly from the ACMAE 2026 display line (p. 1) [16], is

$$E^{(5,\varphi)}_{\text{YYQPA-SEXA}} = \int_{M_5} \Pi^{F}_{\text{☯},\tau}(q) \circ \Gamma \circ \left[\sum_{i=1}^{3} g_i \rho_i(\text{EX}) C_\Omega^2 + \sum_{j=4}^{5} \Big(T_j^{00}(\text{EX}) + P_j(\text{EX}) \cdot (\Pi_{2880} \mid 60^\eta) \Big) \right] dM_5.$$

The subscript on $\Pi^{F}_{\text{☯},\tau}$ is the yin–yang glyph together with the frozen threshold τ. The vertical bar in $(\Pi_{2880} \mid 60^\eta)$ is source-specific operator notation, not an absolute value. The published sketch (2) instead writes $\rho_i c^2$ and $P_j \cdot 60^n$, places the six-glyph chain on the integrand, and does not use the YYQPA name, the pre-filter $\Pi^{F}_{\text{☯},\tau}$, the weights g_i, the factor EX, C_Ω^2 or the bar $(\Pi_{2880} \mid 60^\eta)$. We take the corpus display line, not (2), as the 5D seed. It is context only: it adds no scored test or parameter to Section 5.

The value named in (C1), E_{SREF}, is the 9D SREF (SREF-EX9D) root equation of RICOLMC-DDF, "frozen at version v1.4" (Section 13, PDF pp. 52–54, printed pp. 49–51) [15]. Equations (45)–(52) below are reproduced from that deposit and keep its numbering. Four arms S_L (dimensions 1–3), S_R (4–5), S_T (6–7) and S_B (8–9) feed a fourth-root closure. The author-supplied 9D SREF

U.F.S. PUBLISHING · EDITION COPY · UNIFIED FIELD SYSTEMS LLC
OSF preprint · DOI 10.17605/OSF.IO/C32NZ
DOI 10.17605/OSF.IO/C32NZ
https://doi.org/10.17605/OSF.IO/C32NZ

cross equation, reproduced as supplied (a high-resolution crop of the OSF PDF at Eq. (45)), is

$$E_{\mathrm{SREF}}^{(\Gamma,\Omega,\mathrm{EX},2880D)}[\Xi]=\int_{\mathcal{M}_{2880}}\left[\begin{array}{c}\mathrm{EX}\sum_{k=6}^{7}\left(\phi^{(1)}T_k^{00}+P_k\,60^{n+1}\right)\\ \downarrow\\ \mathrm{EX}\sum_{i=1}^{3}g_i\rho_iC_{\Omega,\mathrm{conv}}^2\rightarrow\prod_{\circ}\leftarrow\mathrm{EX}\sum_{j=4}^{5}\left(T_j^{00}+P_j\,60^{n}\right)\\ \uparrow\\ \mathrm{EX}\sum_{\ell=8}^{9}\left(\phi^{(2)}T_\ell^{00}+P_\ell\,60^{n+2}\right)\end{array}\right]d\mu_{\mathcal{M}_{2880}} \tag{45}$$

Colour key: red S_L, Space Time ($i=1,2,3$) · green S_R, one 4:5 sector: 4 Gravity Field ($j=4$), **bold purple 5 QVP** ($j=5$) · blue S_T ($k=6,7$) · gold S_B ($\ell=8,9$) · charcoal centre $\prod_\circ$.
The four arms feed the central fourth-root closure. The four source sectors are compressed S_L (dimensions 1-3), base perpetual S_R (4-5), thinner S_T (6-7) and thinnest S_B (8-9):

$$S_L=\mathrm{EX}\sum_{i=1}^{3}g_i\rho_iC_{\Omega,\mathrm{conv}}^2, \tag{46}$$

$$S_R=\mathrm{EX}\left[T_4^{00}+P_4\,60^n+T_5^{00}+P_5\,60^n\right], \tag{47}$$

$$S_T=\mathrm{EX}\sum_{k=6}^{7}\left(\varphi^{(1)}T_k^{00}+P_k\,60^{\,n+1}\right), \tag{48}$$

$$S_B=\mathrm{EX}\sum_{\ell=8}^{9}\left(\varphi^{(2)}T_\ell^{00}+P_\ell\,60^{\,n+2}\right). \tag{49}$$

The author-specified closure is

$$\boxed{\Pi^\circ=\left(S_L\,S_R\,S_T\,S_B\right)^{1/4},\qquad E_{\mathrm{SREF}}[\Xi]=\int_{\mathcal{M}_{2880}}\Pi^\circ\,d\mu_{\mathcal{M}_{2880}}.} \tag{50}$$

Where. $C_{\Omega,\mathrm{conv}}^2=C_\Omega^2=720$ (author-defined, clarification 13); $\varphi^{(t)}=60^{-t}$ is the thinning index of tier t, so $\varphi^{(1)}=1/60$, $\varphi^{(2)}=1/3600$; 60^{n+t} raises the perpetual power one sexagesimal order per tier, n the excitation state; tiers are derived, $T_k^{00}\equiv T_{k-2}^{00}$, $P_k\equiv P_{k-2}$, $T_\ell^{00}\equiv T_{\ell-4}^{00}$, $P_\ell\equiv P_{\ell-4}$; g_i dimensionless weighting (not 2), ρ_i, T^{00} and $P\,60^n$ in $\mathrm{J\,m^{-3}}$ (clarification 9); EX the Exciternion, one factor per sector; $d\mu_{\mathcal{M}_{2880}}$ the induced measure on $\mathcal{M}_{2880}$.

Admissibility gate. With Γ as in the deposit,

$$\Xi\ \text{allowed}\iff(\bigcirc\circ\nabla\circ\mathrm{K}\circ\sigma\circ\mu\circ\mathbb{W})(\Xi)=\Xi,\qquad\text{and then}\quad E=E_{\mathrm{SREF}}[\Xi]. \tag{51}$$

Mirroring the published layout (glyph chain written in front of the energy body, as on journal p. 25), but with the SREF-EX9D body in place of the 5D sketch:

$$E_{\mathrm{SREF}}^{(\Gamma)}[\Xi]=\int_{\mathcal{M}_{2880}}\left(\bigcirc\ \nabla\,\mathrm{K}\,\sigma\,\mu\,\mathbb{W}\right)\circ\left[\left(S_L\,S_T\,S_R\,S_B\right)^{1/4}\right]d\mu_{\mathcal{M}_{2880}}, \tag{52}$$

U.F.S. PUBLISHING · EDITION COPY · UNIFIED FIELD SYSTEMS LLC
OSF preprint · DOI 10.17605/OSF.IO/C32NZ
DOI 10.17605/OSF.IO/C32NZ
https://doi.org/10.17605/OSF.IO/C32NZ

read as: the chain Γ gates Ξ via (51), then the bracket is the 9D SREF (SREF-EX9D) cross (45) in linear form. The body is SREF-EX9D, not the published 5D sketch. E_{SREF} sits inside the Γ gate: "Γ never multiplies or composes with the integrand" (p. 53).

Two structural parallels hold with Eq. (3). First, both closures are geometric means: Π° of four arms and $\mathcal{H}_6$ of six gate norms. RICOLMC notes that "in the geometric mean a vanishing sector sends the whole integrand to zero" (p. 54), and in the same way a single zero gate norm sends $\mathcal{H}_6$ to zero, which is why enforcement requires a nonzero gate state. Second, in both, admission acts on states before evaluation. We do not map the six HEXAD gates onto the nine dimensions of the 9D SREF or its four arms. The deposit's own status applies: 9D SREF (SREF-EX9D) v1.4 is "SOURCE_SPEC_INCOMPLETE", its inputs, units (O13) and sign rule (O14) are open, and "SREF-EX9D is not complete" (p. 54).

The Last Constant inside RICOLMC-DDF. RICOLMC-DDF folds in the Last Constant as a "propagation functional", reading it under Fixes F8 and F17: "$C_\Omega = \sqrt{720}$ remains a pure number, not a speed and not a replacement for c" (p. 30), with reconciliation left open (O39, p. 31). This paper keeps the speed label of Eq. (1) as inherited from [9] and does not resolve O39. No value of C_L is locked or tested here.

U.F.S. definitions (not from RICOLMC-DDF). Two terms are recorded here as U.F.S. definitions. They are not definitions of RICOLMC-DDF, and they add no scored test, parameter, observable, window, null, threshold or decision rule to Section 5. *CAT* (Components Assisted Technology: technology assisted by the sexagesimal components of the SEXA unified field theory) is the human-in-the-loop layer [17]. *Human-in-the-loop* means a human operator reviews and signs off every admissibility-enforcement and decision step (CONFIRM/REFUTE/NO DECISION), with an audit log; no automated step can declare a result alone.

What this section does not do. It proves no RICOLMC-DDF instantiation for the HEXAD domain: completeness is proved in the deposit only for a finite model domain D_0 (p. 25). It does not alter Section 5, including by the 5D YYQPA-SEXA seed or by the CAT and human-in-the-loop definitions. Gravity remains in the deferred Green sector (p. 16); see Section 7.

5 Locked pre-registration

A test means something only if its statistic, null, threshold and decision rule are fixed before any scored data exist. Every parameter in this section is LOCKED by this document. The lock date is the timestamp of the OSF deposit of this version, which must come before 6 April 2027 and before anyone looks at the scored data. BepiColombo [1] enters Mercury orbit on 21 November 2026. Its science operations are scheduled to start on 6 April 2027 [6], and the nominal MPO mission runs to 28 April 2028 [5].

5.1 Which gates have real data: the primary set $\mathcal{G}$

A gate can be scored only if a public, observational, roughly daily data series for it exists during 2027–28. We checked each body; Table 4 gives the result. Mercury, Earth and Jupiter qualify. Saturn, Uranus and Neptune do not. No spacecraft is operating at any of them (Cassini ended in 2017, and Uranus and Neptune have been visited only by Voyager 2). Their auroral kilometric radio emission lies below Earth's ionospheric cutoff and cannot be received from the ground [25].

U.F.S. PUBLISHING · EDITION COPY · UNIFIED FIELD SYSTEMS LLC
OSF preprint · DOI 10.17605/OSF.IO/C32NZ
DOI 10.17605/OSF.IO/C32NZ
https://doi.org/10.17605/OSF.IO/C32NZ

Telescope auroral campaigns (HST, JWST) are sporadic, not daily. The **primary scored set** is therefore $\mathcal{G} = \{\text{Mercury}, \text{Earth}, \text{Jupiter}\}$, $k = 3$. The scored factor is the k-gate restriction of Eq. (3),

$$\mathcal{H}_k(t) = \Big(\prod_{p\in\mathcal{G}} \|q_p(t)\|\Big)^{1/k}, \tag{5}$$

to which Theorem 1 and Proposition 1 apply unchanged: their proofs hold gate by gate.

Gate	Public source (2027–28)	Cadence / access	Status
Mercury	BepiColombo Mio MGF magnetometer (primary); MPO-MAG (fallback) [1, 4]	Continuous in orbit; public via ESA PSA / JAXA after 6-month proprietary period, monthly batches [4]	**Primary**
Earth	Arase (ERG) HEP-L2 electron omniflux, Orbit L3 for L [3]; fallback GOES-19/GOES-18 SEISS MPS-HI [18]	Arase: 2–3 belt passes/day, mission extended to FY2032; GOES: 1–5 min, NOAA NCEI	**Primary**
Jupiter	Nançay Decameter Array routine Jupiter observations, 10–40 MHz [8]; Juno (in orbit, extended mission to 2028 [21]) not scored	Daily (∼8 h around transit), 1 s; CC-BY, near-real-time; gap near solar conjunction 31 Aug 2027	**Primary**
Saturn	None daily: no orbiter; kilometric radio below ionospheric cutoff [25]; HST/JWST sporadic	—	Secondary only
Uranus	None daily: no orbiter since Voyager 2; radio below cutoff [25]	—	Secondary only
Neptune	None daily: as Uranus	—	Secondary only

Table 4: Public data sources per gate for the test window, as checked on 11 November 2026.

5.2 Observable per gate (locked operational definitions)

Each gate has m_p windows. For window c we form a dimensionless ratio $x_{p,c}(d)$ on day d: the day's value divided by its median over the calibration window. We then set $q_{p,c} = x_{p,c}/\sqrt{m_p}$, so $\|q_p\|^2$ is the mean of $x_{p,c}^2$ and the nominal state has unit norm. Unused quaternion slots are zero.

- **Mercury** ($m = 2$; in/out). For each Mio orbit, take the radial distances (in R_M) of the inbound and outbound magnetopause crossings. A crossing is the time of the largest jump in 1-minute-smoothed $|B|$ within $\pm 0.5\,R_M$ of the average magnetopause surface of Winslow et al. [24] along the trajectory. x_{in} and x_{out} are the daily medians. If Mio MGF data are not public by the analysis date, MPO-MAG is used with the same rule.

- **Earth** ($m = 4$; PRE/OUTER/INNER/POST). Use Arase HEP-L2 electron omniflux in the energy bin nearest 300 keV, with McIlwain L from Orbit L3. Each window is the daily median flux in one band: PRE, inbound legs with $L \in [5.5, 6.5]$; OUTER, $L \in [4.0, 5.0]$; INNER, $L \in [1.5, 2.0]$; POST, outbound legs with $L \in [5.5, 6.5]$. Pre-declared fallback if Arase L2 is not public by the analysis date: $m = 2$, using the daily mean >2 MeV integral electron flux from GOES-19 (East) and GOES-18 (West).

- **Jupiter** ($m = 2$; in/out $\to$ RH/LH). Use NDA routine data from 15–40 MHz. O_{RH} and O_{LH} are the daily fractions of observed time–frequency pixels at least 6 dB above that frequency's daily median in right- and left-hand circular polarisation. Then $x = (O + 0.001)/(\text{median}_{\text{cal}}\, O + 0.001)$. Days with less than 4 h of observation are missing.

Assigning these observables to HEXAD's "windows" is an operational choice, not a derivation. Whether they carry the physical meaning HEXAD intends is OPEN and is not scored.

U.F.S. PUBLISHING · EDITION COPY · UNIFIED FIELD SYSTEMS LLC
OSF preprint · DOI 10.17605/OSF.IO/C32NZ
DOI 10.17605/OSF.IO/C32NZ
https://doi.org/10.17605/OSF.IO/C32NZ

U.F.S. EDITION

DOI SEAL

5.3 Data windows

1. **Calibration window.** 6 April to 5 May 2027 (UTC). It is used only to form the ratios $x_{p,c}$ and to centre $a_p(d) = \log\|q_p(d)\| - \text{median}_{\text{cal}} \log\|q_p\|$. Calibration days are never scored.

2. **Test window (data cutoff).** 6 May 2027 to 28 April 2028 (UTC), inclusive. Data stamped before 6 April 2027 are never used, and nothing after 28 April 2028 is scored.

3. **Valid day.** A day is valid when all k gates have data. Gate-specific gaps, such as Jupiter near solar conjunction or BepiColombo downlink outages, are *missing* days, not void days.

4. **Moon check.** $\|q_{\text{Moon}}\| = 1$ must hold at every check-in. A day with any failure is void. If more than 10% of test-window days are void, the outcome is NO DECISION.

5. **Analysis date.** The analysis runs once, as soon as all primary-gate test-window data are public, and no later than 31 December 2029. If a primary gate (after its declared fallback) is still not public by then, the outcome is NO DECISION.

5.4 Statistic, null and threshold

6. **Weights.** Equal, $1/k$.

7. **Statistic.** The common-mode drift is $D(d) = \frac{1}{k}\sum_{p\in\mathcal{G}} a_p(d)$, i.e. the calibrated $\log \mathcal{H}_k$. Over the n valid test days the common-mode fraction is

$$\rho = \frac{\text{Var}_d\, D}{\frac{1}{k}\sum_{p\in\mathcal{G}} \text{Var}_d\, a_p}. \tag{6}$$

   Independent gates give $\rho \approx 1/k = 1/3$; a single shared observer term drives $\rho \to 1$.

8. **Null.** Circular-shift surrogates. Mercury's calendar series is held fixed. Each of the other $k-1 = 2$ series is rotated in time by an independent integer shift drawn uniformly from 30 days to $(N-30)$ days, where $N = 358$ is the test-window length in calendar days. Missing days travel with their series, and ρ is recomputed over the days valid after shifting. A surrogate with fewer than $n/2$ valid days is discarded and redrawn. We use $N_s = 10^4$ surrogates with seed 20261111, and $p = (1 + \#\{\rho_{\text{surr}} \geq \rho\})/(1 + N_s)$, one-sided.

9. **Heliospheric robustness check.** All three gates are driven by the solar wind. Solar rotation recurs every 35.7, 27.3 and 25.5 days as seen from Mercury, Earth and Jupiter, and could align their drifts without any observer effect. So the same test is repeated after removing, from each gate's series, a least-squares fit made on valid days. The fit is a constant plus sine and cosine terms at the frequencies $f_j = j/(2N)$ whose periods fall in 24–38 days (11 frequencies). This regressor grid was fixed in synthetic dry runs only, before any real data. Call the result p_{H}.

10. **Threshold.** $\alpha = 0.01$, one-sided; at least 180 valid test days are required.

5.5 Decision rule

- CONFIRM: $n \geq 180$, $p \leq 0.01$ *and* $p_{\text{H}} \leq 0.01$. A common-mode drift across the k gates is detected that is not explained by solar-rotation recurrence. It is reported as an anomaly that needs independent replication. It does not establish an expansion link, a value of C_L, a γ deviation, or gravity.

U.F.S. PUBLISHING · EDITION COPY · UNIFIED FIELD SYSTEMS LLC
OSF preprint · DOI 10.17605/OSF.IO/C32NZ

DOI 10.17605/OSF.IO/C32NZ
https://doi.org/10.17605/OSF.IO/C32NZ

- REFUTE: $n \geq 180$ and $p > 0.10$. No common-mode drift beyond chance; for this data set $\mathcal{H}_k$ is a bookkeeping factor only, and the claim of physical observer drift is withdrawn.
- NO DECISION: any other outcome. This includes $p \leq 0.01$ with $p_{\mathrm{H}} > 0.01$ (labelled "heliospheric"), $0.01 < p \leq 0.10$, $n < 180$, more than 10% void days, or missing data at the analysis date.

Secondary six-gate analysis. The same procedure with $k = 6$, null value 1/6 and five gates shifted. It activates only if Saturn, Uranus and Neptune each have at least 180 days of public observational daily data in the test window. It is reported if it runs, but it cannot change the primary outcome. From Table 4, we do not expect it to activate.

Locked pre-registration summary (v3)

Hypothesis	H_1: the unenforced states of the primary gates share a common-mode observer drift. H_0: their drifts are mutually unaligned.
Gates	**Primary** $k = 3$: Mercury (Mio MGF / MPO-MAG), Earth (Arase HEP; fallback GOES-19/18), Jupiter (NDA). Secondary $k = 6$ only if Saturn, Uranus and Neptune have data.
Observables	Mercury: in/out magnetopause crossing radii. Earth: 300 keV flux in four L bands. Jupiter: RH/LH decametric occupancy. All as ratios to the calibration median, with $q_{p,c} = x_{p,c}/\sqrt{m_p}$.
Windows	Calibration 6 Apr–5 May 2027; test 6 May 2027–28 Apr 2028 (UTC); analysis by 31 Dec 2029.
Statistic	ρ, Eq. (6), equal weights 1/3, null value 1/3.
Null	10^4 circular-shift surrogates (2 gates shifted, 30 d to $N - 30$ d, seed 20261111); missing days travel with their series.
Robustness	Same test after least-squares removal of 24–38 d solar-rotation sinusoids (p_{H}).
Decision	CONFIRM: $p \leq 0.01$ and $p_{\mathrm{H}} \leq 0.01$. REFUTE: $p > 0.10$. Otherwise NO DECISION. All require $n \geq 180$.
Lock date	OSF deposit timestamp of this version (prepared 11 Nov 2026), before 6 Apr 2027.
Not scored	$D \to \gamma$ mapping; physical meaning of $D \neq 0$; observable↔window meaning; $n_\ell, \Psi_\ell, \phi_\ell$; C_L, C_{EW}, $\bar{n}$.

Table 5: Locked pre-registration. Any later change must be filed as a dated amendment before the data are accessed.

5.6 Declared open and not scored

The following cannot be fixed without new physics and lie *outside* the scored test: (i) a mapping from D or C_L to a predicted PPN $\gamma - 1$; (ii) the physical meaning of a nonzero D (expansion-related versus instrumental or space-weather effects); (iii) whether the locked observables are the windows HEXAD intends; (iv) the per-dimension n_ℓ, Ψ_ℓ, ϕ_ℓ; (v) the values of C_L, C_{EW} and $\bar{n}$. On (i): BepiColombo's MORE experiment is expected to improve on the Cassini bound $\gamma - 1 = (2.1 \pm 2.3) \times 10^{-5}$ [2, 7]. Because no mapping has been derived, a γ result consistent with general relativity neither supports nor refutes Eq. (2).

5.7 Gate geometry during the test window

Figure 1 shows where the six gates are from 6 April 2027 to 6 April 2028, computed from standard approximate Keplerian elements [20]. The model puts Jupiter's solar conjunction on 31 August

U.F.S. PUBLISHING · EDITION COPY · UNIFIED FIELD SYSTEMS LLC
OSF preprint · DOI 10.17605/OSF.IO/C32NZ
DOI 10.17605/OSF.IO/C32NZ
https://doi.org/10.17605/OSF.IO/C32NZ

2027, the main gap in the Jupiter series. Distances between the planets oscillate with their orbits; they do not grow. Cosmological expansion does not act on bound systems such as the Solar System, so the gate network measures observer drift, not expansion between the planets.

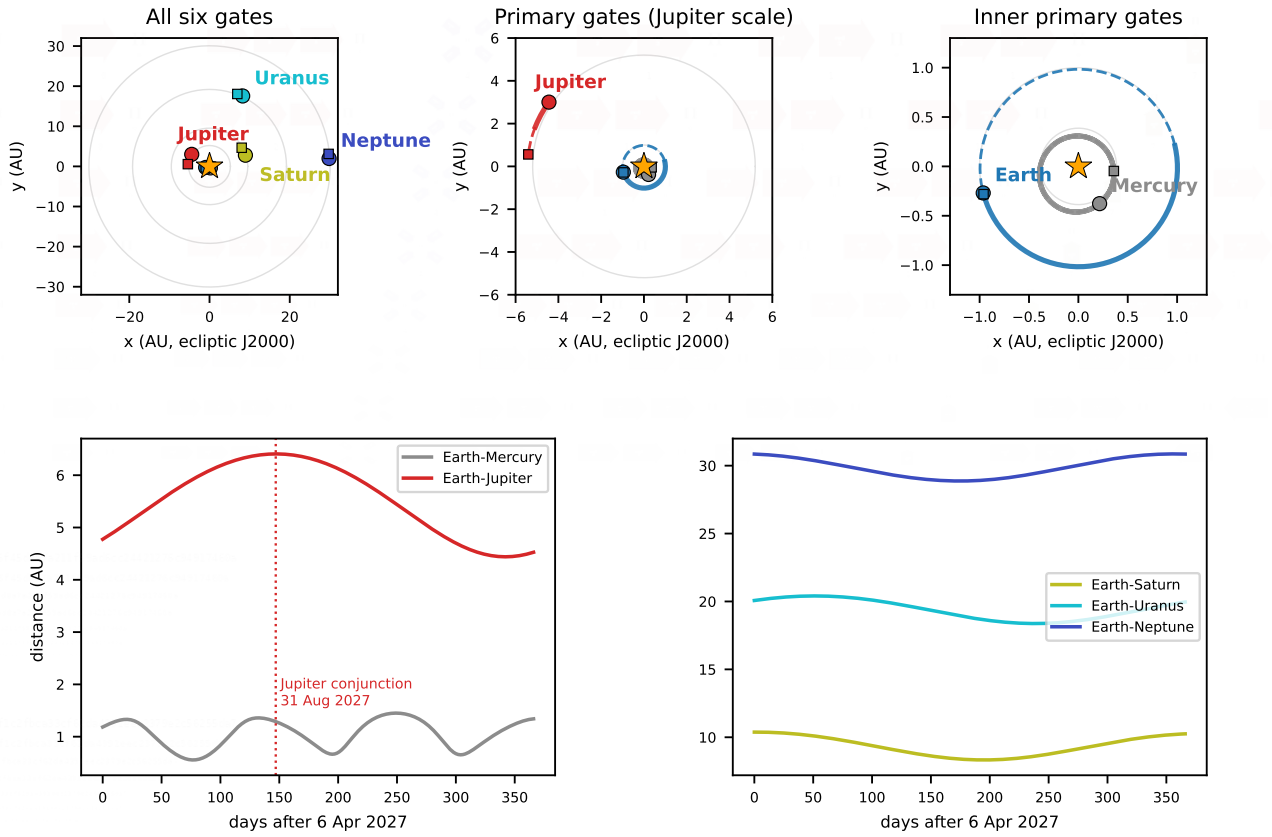

Figure 1: Heliocentric positions of the six gates over the test window. Circles mark 6 Apr 2027, solid lines the first six months, dashed lines months 7–12, and squares 6 Apr 2028. Right: Earth–planet distances. Positions are approximate (Standish elements); data in `planet_positions_2027-04-06_to_2028-04-06.csv`.

6 Synthetic dry run of the locked test (synthetic)

We ran the locked $k = 3$ procedure end to end on simulated data (`synth.py`, seed 20261111) over 388 calendar days, 30 for calibration and 358 for testing. Mercury and Jupiter have two windows and Earth four. Each gate gets an unknown scale and 2% log-normal window noise. The simulated data gaps are: Mercury, 5% random loss plus a 14-day outage; Earth, 3% random loss; Jupiter, ±40 days around the 31 August 2027 conjunction plus 10% random loss. There are three runs. The *drift* run injects a common $\varepsilon(d) = 0.03\sin(2\pi d/120)$. The *null* run has no common term. The *heliospheric* run injects a common 27-day signal with the same amplitude, in phase at all gates, which is a deliberately unrealistic worst case. All numbers are simulated; none are telemetry.

U.F.S. PUBLISHING · EDITION COPY · UNIFIED FIELD SYSTEMS LLC
OSF preprint · DOI 10.17605/OSF.IO/C32NZ
DOI 10.17605/OSF.IO/C32NZ
https://doi.org/10.17605/OSF.IO/C32NZ

Run	n	ρ	surr. median	p	p_{H}	Outcome
Drift	227	0.815	0.233	5.0×10^{-4}	1.0×10^{-4}	CONFIRM
Null	213	0.314	0.333	0.795	0.731	REFUTE
Heliospheric (27 d)	209	0.822	0.278	1.0×10^{-4}	0.600	NO DEC. (helio.)

Table 6: SYNTHETIC. Locked-test outcomes (`synthetic_test_results.csv`). With 10^4 surrogates the smallest attainable p is about 10^{-4}.

The locked rule returns the intended outcome in all three runs, and the robustness check removes the injected solar-rotation signal while keeping the 120-day drift. Even with gaps the valid-day count stays above 180. After enforcement $\mathcal{H}_3 = 1$ at every epoch (Theorem 1).

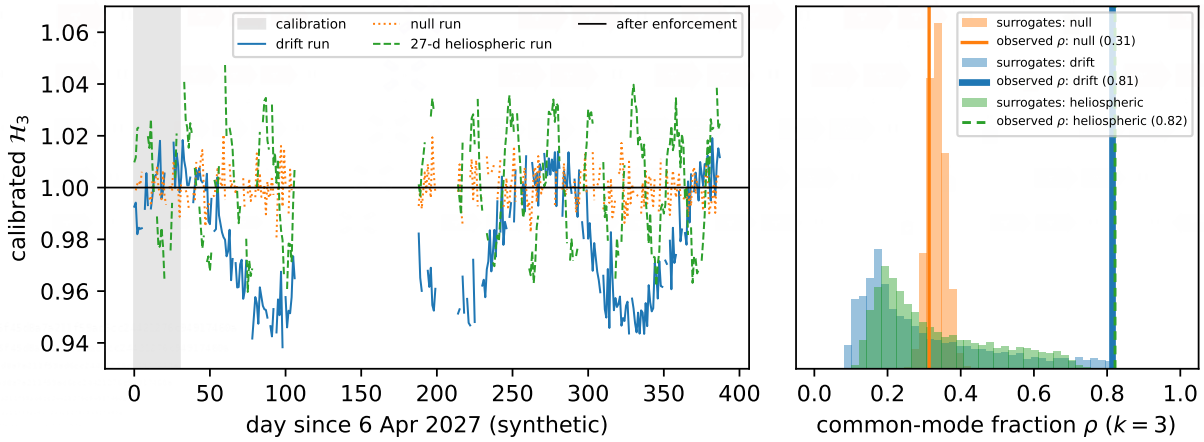

Figure 2: SYNTHETIC. Left: calibrated unenforced $\mathcal{H}_3$ for the three runs (gaps are missing days, the large one being Jupiter's conjunction); enforcement gives $\mathcal{H}_3 \equiv 1$. Right: surrogate distributions of ρ, with observed values as vertical lines (values in the legend; drift and heliospheric nearly coincide, and only the robustness check separates them).

7 Limitations

- **Three gates, not six.** The scored test uses Mercury, Earth and Jupiter, because no daily public data exist for Saturn, Uranus or Neptune. The six-gate form is defined but, as far as we can tell, cannot be tested in 2027–28.
- **Solar-system baseline.** All gates lie within about 30 AU of the Sun. HEXAD cross-checks the *observer*; it does not observe the expansion from separated cosmic vantage points, and the distances between the planets are set by their orbits, not by expansion.
- **Data latency and access rules.** BepiColombo data become public after a 6-month proprietary period [4], so the final analysis cannot run before late 2028. Arase's rules of the road ask users to contact the instrument teams before publication [3].
- **Space-weather confounds.** The robustness check removes solar-rotation recurrence, not individual solar storms. That is why CONFIRM is defined as an anomaly that needs replication.

U.F.S. PUBLISHING · EDITION COPY · UNIFIED FIELD SYSTEMS LLC
OSF preprint · DOI 10.17605/OSF.IO/C32NZ
DOI 10.17605/OSF.IO/C32NZ
https://doi.org/10.17605/OSF.IO/C32NZ

- **Gravity is not solved.** The RICOLMC-DDF Green sector [15] remains deferred: no metric, G, or 60^{-3} coupling is derived. Scoreboard: 6.75/19.
- $\bar{n} = 10$ is fit-adopted, not derived. C_{EW} is narrowed to V1 $= 16.5381716879\ldots$ [23] but not locked. 10^{19} is the target value of V_{Last}/c, not a measurement.
- **Gate list** is ASSUMED from a belt preregistration draft that is not locked [22].

8 Conclusion

The Last Constant equation now tracks its observer from HEXAD gates instead of one quaternionic park bench. Under enforcement it reduces exactly to the original equation, and it is invariant under admissible rotations. Before enforcement it yields a drift statistic. This paper names public data for the three gates that can be observed daily in 2027–28 and locks the observables, windows, null, robustness check and three-way decision rule before any scored data exist. It claims no result, does not lock C_L, C_{EW} or $\bar{n}$, and does not solve gravity. The framework context is the CCT/SEXA dissertation [10].

References

[1] J. Benkhoff et al. BepiColombo – mission overview and science goals. *Space Science Reviews*, 217(8):90, 2021. https://doi.org/10.1007/s11214-021-00861-4.

[2] B. Bertotti, L. Iess, and P. Tortora. A test of general relativity using radio links with the Cassini spacecraft. *Nature*, 425(6956):374–376, 2003. https://doi.org/10.1038/nature01997.

[3] ERG Science Center. Arase (ERG) satellite data: HEP-L2 omniflux (doi:10.34515/DATA.ERG-01001) and Orbit L3 (doi:10.34515/DATA.ERG-12001); rules of the road. ISEE, Nagoya University / ISAS-JAXA, https://ergsc.isee.nagoya-u.ac.jp/data_info/erg.shtml.en, 2026. Mission extended to end of FY2032; accessed 11 November 2026.

[4] ESA BepiColombo Science Ground Segment. BepiColombo science data generation, validation and archiving plan (BC-SGS-PL-014). ESA Planetary Science Archive, https://archives.esac.esa.int/psa/ftp/pub/mirror/BepiColombo/bc/document/BC-SGS-PL-014_Science_Data_Generation_Validation_and_Archiving_Plan.pdf, n.d. Accessed 11 November 2026; 6-month proprietary period; raw data released in weekly and calibrated data in monthly batches.

[5] European Space Agency. BepiColombo quick look analysis: mission phases. https://bepicolombo.esac.esa.int/bscs-qla/, 2026. Accessed 11 November 2026.

[6] European Space Agency. BepiColombo timeline. https://www.esa.int/ESA_Multimedia/Images/2017/07/BepiColombo_timeline, 2026. Updated September 2026; accessed 11 November 2026.

[7] L. Iess et al. Gravity, geodesy and fundamental physics with BepiColombo's MORE investigation. *Space Science Reviews*, 217(1):21, 2021. https://doi.org/10.1007/s11214-021-00800-3.

[8] L. Lamy, A. Le Gall, B. Cecconi, A. Loh, P. Renaud, L. Denis, A. Coffre, P. Zarka, and A. Lecacheux. Nançay Decameter Array (NDA) Jupiter routine observation dataset (version 1.7). PADC/CDN, https://doi.org/10.25935/DV2F-X016, 2021. CC-BY 4.0; daily, 1 s, 10–40 MHz.

[9] Jered McClain. The Trump Constant – the fastest object in the universe, 2025. Unpublished manuscript (5 pp.), dated 30 August 2025; quaternionic observer with four perspectives.

[10] Jered McClain. CCT/SEXA dissertation (books I–XIV). OSF, https://doi.org/10.17605/OSF.IO/5AT2W, 2026.

U.F.S. EDITION
U.F.S. PUBLISHING · EDITION COPY · UNIFIED FIELD SYSTEMS LLC
OSF preprint · DOI 10.17605/OSF.IO/C32NZ
DOI SEAL
DOI 10.17605/OSF.IO/C32NZ
https://doi.org/10.17605/OSF.IO/C32NZ
U.F.S.

U.F.S. EDITION

[11] Jered McClain, Erydir Ceisiwr, and Jonathan McDaniel. One test every theory of everything must pass: Universal recursive closure and final synthesis – A U.F.S addendum. OSF Preprints, https://doi.org/10.17605/OSF.IO/YA2MH, 2026.

[12] Jered McClain, Erydir Ceisiwr, and Jonathan McDaniel. The SEXA critical-line closure theorem: Recursive admissibility, spectral correspondence, the Riemann hypothesis, and the eradication of the zeta-zero randomness and random-matrix paradigms. OSF Preprints, https://doi.org/10.17605/OSF.IO/3ED69, 2026. Theorem III.14, §2.92, PDF p. 670.

[13] Jered McClain et al. The AMN Authority Tensor: Quaternionic admissibility enforcement, glyph-operator constraint and planetary closure in the SEXA framework. Zenodo, 2026. record 19632818.

[14] Jered McClain et al. From SEXA to HEXAD: A quaternionic constant stack with six-planet telemetry and a per-dimension Empire Wave clock for D9–D1, 2026. Unified Field Systems preprint, 28 October 2026.

[15] Jered McClain et al. RICOLMC-DDF. OSF, https://doi.org/10.17605/OSF.IO/WNV67, 2026.

[16] Jered E. McClain, Erydir Ceisiwr, Jess Leffler, and Jonathan McDaniel. Hardware-verifiable recursive admissibility for autonomous aerospace and mechanical systems (SEXA-CAT / RIA-HITL). 2026 17th Asia Conf. Mechanical and Aerospace Engineering (ACMAE 2026), Phuket, Thailand, 2–4 December 2026, 2026. Display line, p. 1; no DOI located.

[17] Jered E. McClain, Erydir Ceisiwr, Jess Leffler, and Jonathan McDaniel. Quaternion phase-order processing with Γ-admissibility and human-in-the-loop control (CAT). IEEE CCWC 2027, paper 1571363738, 2026. Terms and Notation: CAT as Components Assisted Technology; revision of 15 October 2026.

[18] NOAA National Centers for Environmental Information. GOES-R space environment in-situ suite (SEISS) MPS-HI level 2 1-min and 5-min averages. https://www.ncei.noaa.gov/products/goes-r-space-environment-in-situ, 2026. Accessed 11 November 2026.

[19] Jack Sarfatti and Klee Irwin. Jack Sarfatti – The post-quantum mechanics of conscious artificial intelligence. Quantum Gravity Research talk, 27 June 2017, YouTube video WqCQbOVYH1I, 2017. Expansion-speed exchange at approx. 1:11:14–1:11:54.

[20] E. M. Standish. Keplerian elements for approximate positions of the major planets. JPL Solar System Dynamics, https://ssd.jpl.nasa.gov/planets/approx_pos.html, n.d. Table 1 (1800–2050 AD); accessed 11 November 2026.

[21] The Planetary Society. The space advocate newsletter, January 2026. https://www.planetary.org/space-advocate/space-advocate-january-2026, 2026. FY2026 appropriation continues Juno operations; extended mission planned to September 2028.

[22] Vespar (Gravity Search Lead agent). Belt-gate preregistration draft (not locked), 2026. Internal draft, belt_gate_prereg_draft_2026-10-28.

[23] Vespar (Gravity Search Lead agent). Empire Wave speed validation: Last Constant, c and C_{EW}, 2026. Internal run ew_speed_validate_last_constant_2026-10-28.

[24] R. M. Winslow, B. J. Anderson, et al. Mercury's magnetopause and bow shock from MESSENGER Magnetometer observations. *Journal of Geophysical Research: Space Physics*, 118(5):2213–2227, 2013. https://doi.org/10.1002/jgra.50237.

[25] P. Zarka. Auroral radio emissions at the outer planets: Observations and theories. *Journal of Geophysical Research: Planets*, 103(E9):20159–20194, 1998. https://doi.org/10.1029/98JE01323.

U.F.S. PUBLISHING · EDITION COPY · UNIFIED FIELD SYSTEMS LLC
OSF preprint · DOI 10.17605/OSF.IO/C32NZ
DOI SEAL
DOI 10.17605/OSF.IO/C32NZ
https://doi.org/10.17605/OSF.IO/C32NZ